Remote Sensing of Environment 239 (2020) 111631

Contents lists available at ScienceDirect

Remote Sensing of Environment

journal homepage: www.elsevier.com/locate/rse

Impact of water characteristics on the discrimination of benthic cover in and around coral reefs from imaging spectrometer data

Tom W. Bell[a,*], Gregory S. Okin[a], Kyle C. Cavanaugh[a], Eric J. Hochberg[b]

[a] Dept. of Geography, University of California, Los Angeles, Los Angeles, CA 90095, USA
[b] Bermuda Institute of Ocean Sciences, St. George's, Bermuda

ARTICLE INFO

Edited by Menghua Wang

ABSTRACT

Coral reefs are the foundation of productive ecosystems in the global, tropical oceans and are under threat from a variety of local to global scale stressors. Satellite imagery provides a tool to identify and understand the processes that control coral reef degradation, however due to the dynamic nature of seawater constituents, current spaceborne multispectral sensors cannot reliably discriminate between the many coral reef benthic classes necessary to detect change. Hyperspectral imagers may provide sufficient spectral resolution to estimate water column properties and differentiate benthic classes, however, the effects of depth, seawater constituents, and classification algorithm on the accuracy of benthic classifications have not been systematically assessed. Here, we simulate the ability of a spaceborne hyperspectral imager to accurately map fractional cover of coral reef benthic classes under a variety of conditions. Benthic reflectance is simulated by combining pure reflectance spectra of coral, algae, and sand and projecting these mixed spectra through a fully crossed set of water columns. We then use a semi-analytical optimization procedure to estimate the water column properties and multiple endmember spectral mixture analysis to estimate the fractional cover of the benthic classes using many independent endmember spectra. We compare our estimated benthic class fractions to the original, actual fractions used to produce the mixed coral reef spectra to quantify several measures of error. We found that multiple endmember spectral mixture analysis decreases fractional retrieval error, which is also reduced when the first derivative of the mixed and endmember spectra is used prior to unmixing. The estimation of fractional benthic class cover is most accurate for depths ≤ 3 m for most water conditions. Depths ≥ 5 m should be classified only if chlorophyll and sediment concentration are < 0.1 mg m^{-3} and < 0.1 g m^{-3}, respectively. Our results indicate that the fractional cover of coral and algae should be at least 25% for accurate benthic class estimates (mean relative error $<$ 50%), however there will be many ways to leverage the repeat measurements of a hyperspectral satellite sensor, such as a stable depth retrievals and benthic cover estimates, to produce more accurate and useful fractional cover data. We show how this simulation analysis can be used to generate maps of predicted benthic cover fractional retrieval uncertainty across a coral reef system using aerial hyperspectral imagery acquired over Hawaii, USA, although reef-specific, within pixel variations in depth and benthic class complexity should be considered.

1. Introduction

Coral reefs form important ecosystems in the global, tropical oceans. These systems are responsible for coastal productivity in oligotrophic waters, support a variety of organisms, and are important for human subsistence and economies. However, coral reef ecosystems are under threat from warmer and more acidic oceans, storms, overfishing, pollution, disease, and predator outbreaks (Dollar and Tribble, 1993; Hughes, 1994; Anthony et al., 2011; Kayal et al., 2012; Smith et al., 2016). Continuous, large-scale monitoring of coral reef benthic community structure is key to understanding the processes that control coral reef degradation (Goodman et al., 2013).

Spaceborne sensors offer a path forward for global, repeat estimates of coral reef attributes, such as coral cover, bleaching events, and macroalgal blooms (*reviewed in* Hedley et al., 2016; Purkis et al., 2019). However, current spaceborne multispectral sensors lack the spectral resolution to discriminate between many benthic classes in a typical reef community (Mumby et al., 1997; Hochberg and Atkinson, 2003).

* Corresponding author.
E-mail addresses: tbell@ucsb.edu (T.W. Bell), okin@geog.ucla.edu (G.S. Okin), KCavanaugh@geog.ucla.edu (K.C. Cavanaugh), eric.hochberg@bios.edu (E.J. Hochberg).

https://doi.org/10.1016/j.rse.2019.111631
Received 19 August 2019; Received in revised form 11 December 2019; Accepted 31 December 2019

An analysis of field measured reflectance spectra of twelve fundamental coral reef benthic classes found that the placement of several well-defined, narrow spectral bands can drastically improve classification accuracy (Hochberg et al., 2003). Thus, measurement of coral reef reflectance using the contiguous, narrow bands of a hyperspectral sensor at appropriate spatial resolution may allow for the detection of distinct spectral features, reducing the need for ancillary data in reef mapping (Hochberg and Atkinson, 2003). In addition, derivative spectra can be calculated from hyperspectral data, which can be used to examine spectral features in a way that is less affected by variability in illumination condition (Tsai and Philpot, 1998). A global, repeat, hyperspectral measurement approach has been recommended by the Decadal Survey for Earth Science Application from Space, with foundational objectives such as determining the functional traits of near-coastal aquatic ecosystems (National Academies of Sciences, Engineering, and Medicine, 2018; Lee et al., 2015; Hochberg et al., 2015). The discrimination of coral reef benthic class cover fits well within the priorities of the Surface Biology and Geology designated observable (SBG).

A fundamental challenge in remotely discriminating coral reef bottom type is deriving the benthic reflectance signal, which is reduced and altered by scattering and absorption in the overlying water column (Holden and LeDrew, 2002). The impact of the water column on benthic reflectance is determined by properties such as chlorophyll, sediment, and colored dissolved organic matter (CDOM) concentrations, which are highly variable across global coral reefs and may vary depending on tidal state and season (Hedley et al., 2012; Russell et al., 2019). As a result, there have been a number of efforts to estimate water column characteristics directly from imagery, so that the bottom reflectance signal can be inferred. These approaches include semi-analytical methods (Lee et al., 1999), look-up tables (Mobley et al., 2005; Hedley et al., 2009), and Bayesian models (Thompson et al., 2017). Almost all of these approaches require imagery with high spectral resolution in order to differentiate between the many potential combinations of water column properties.

While these approaches indicate potential for accurately mapping coral reef community structure from hyperspectral imagery (e.g. Goodman and Ustin, 2007; Thompson et al., 2017), there is still uncertainty about how water column properties impact error in benthic cover estimates. For example, modeling studies by Kutser et al. (2003) and Lubin et al. (2001) suggest that most coral reef bottom types can be distinguished up to depths of 5–10 m, but these studies assumed clear water. Thompson et al. (2017) implemented a novel Bayesian approach for retrieving benthic reflectance spectra in varying water conditions with both 'clear' and 'turbid' water conditions, although seawater conditions can be more turbid than these scenarios. Hedley et al. (2012) examined how a suite of sensor and environmental variables, including five different inherent optical property (IOP) classes over six depth combinations, could affect the spectral separation of hyperspectral data to identify the primary factors which confound the discrimination of mixed coral reef spectra. Garcia et al. (2018) developed an improved inversion technique that selects a bottom spectrum from remote sensing reflectance before IOPs and specific benthic classes are estimated. However, as the individual effects of IOPs were not the focus of the study, the accuracy of this procedure was averaged across a range of simulated scattering and absorption values. A more comprehensive and independent assessment of individual water properties could be used to quantify uncertainty in image classifications and identify in greater detail the combination of depth and water column constituents that prohibit accurate benthic cover classifications.

Medium spatial resolution satellite imagery (10–30 m) also poses a challenge for coral reef observation as multiple benthic classes (live and bleached coral, various algal species, sand) usually exist within a typical remote sensing pixel (Andréfouët et al., 2002). Estimating the fractional cover of each benthic class inside a pixel would aid in understanding change in reef composition through time (Thompson et al., 2017). Spectral mixture analysis (SMA), the modeling of mixed pixels using "pure" spectral endmembers, is probably the most common method for estimating subpixel fractional coverage (*reviewed in* Somers et al., 2011). SMA has been used to estimate fractional cover of different coral reef benthic classes in the past by using only a single representative coral, algal, and sand spectral endmember, without the confounding effects of a water column, under ideal ocean conditions, or without rigorous site-based validation (Hochberg and Atkinson, 2003; Hedley et al., 2004; Goodman and Ustin, 2007). The use of multiple, diverse spectral endmembers for each benthic class may prove more accurate as benthic classes can be spectrally variable (Hochberg et al., 2003; Thompson et al., 2017). Multiple endmember spectral mixture analysis (MESMA) utilizes multiple class-specific, representative spectral endmembers to iteratively model each pixel and determine the optimal combination of endmember fractions (Roberts et al., 1998). In other complex ecosystems, this technique has shown improvements over single endmember SMA (Okin et al., 2013; Okin and Gu, 2015; Meyer and Okin, 2015).

Here we describe a simulation analysis where we use known fractional combinations of coral reef benthic classes to examine the potential benefits of MESMA and spectral derivatives in reducing the fractional retrieval error for spectrally complex benthic classes. We also examine the benthic class fractional retrieval error under a diverse and fully crossed set of water columns and investigate how the absorption and scattering properties of water column constituents and depth influence benthic class separability. We investigate the confusion between benthic classes and the minimum fractions detectable under various water column conditions. Finally, we use aerial hyperspectral imagery collected over Hawaii, USA to produce maps of predicted fractional retrieval uncertainty based on the estimated water column properties. While the within pixel complexities of natural coral reefs should always be considered, such as benthic class patchiness and depth variability, this study delivers a set of water column properties which should lead to reduced uncertainty when estimating benthic class fractional cover using global scale hyperspectral imagery made available by a future spaceborne imaging spectrometer.

2. Methods

2.1. Overview

In order to simulate reflectance spectra of the many combinations of benthic classes found on a coral reef, we created spectral mixtures using field collected reflectance spectra of individual benthic classes (Hochberg et al., 2003; Fig. 1, Step 1). The fractions used to make these endmembers represented 'truth' against which retrieved fractions were compared to calculate fractional cover error. In brief, these benthic mixtures (Fig. 1, Step 2) were passed through simulated water columns combining a variety of absorption and scattering characteristics to estimate the above-water surface reflectance of each spectral mixture/water column combination (Fig. 1, Step 3). Water column properties were then estimated from the above-water reflectance in Step 3 using a semi-analytical optimization model. These estimated properties were then used to produce a new simulated water column which was then applied to remaining spectral endmembers for each benthic class (Fig. 1, Step 4). These spectral endmembers represent pure benthic class bottom types as viewed through a water column and were used to unmix the above-water surface reflectance of the spectral mixture formed in Step 3 using MESMA (Fig. 1, Step 5). The fractional cover of each benthic class estimated by MESMA was then compared to the original, actual fractional cover used to produce the mixed spectrum and fractional cover estimation error was calculated. These steps are described in detail below.

2.2. Spectral mixtures of coral reefs

The spectra used for the simulation of benthic reflectance included

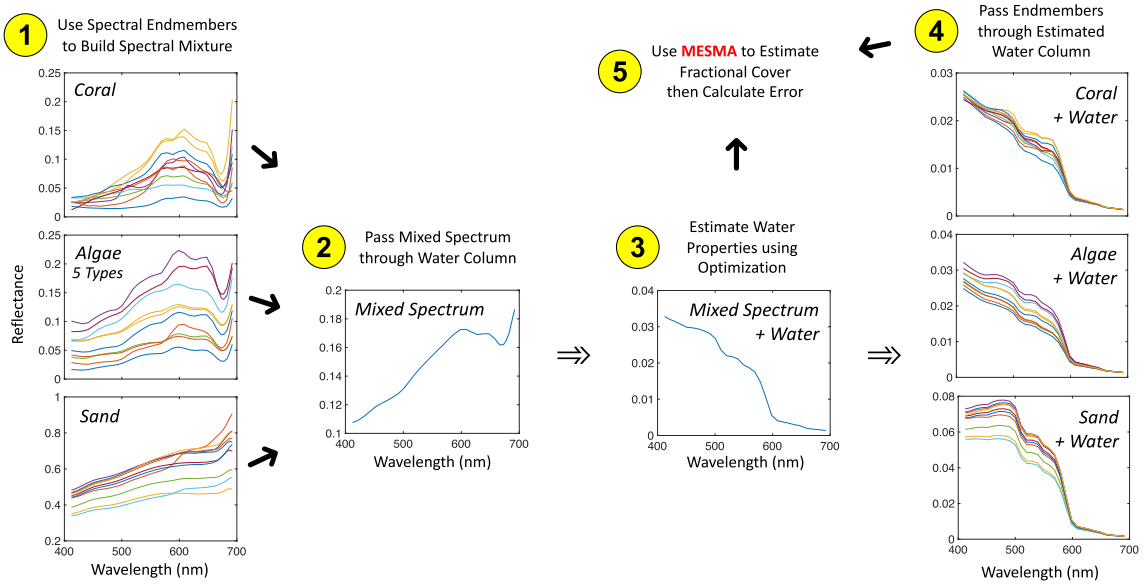

Fig. 1. Schematic showing the process used to quantify error in estimated fractional cover under various water column properties. 1. One of ten field measured reflectance spectra for each bottom class (Live Coral, Algae, Sand) was selected. 2. The selected endmember spectra were then combined linearly in one of 48 fractional combinations to create a simulated 'coral reef reflectance spectrum'. 3. This mixed spectrum was then passed through simulated water columns combining a variety of absorption and scattering characteristics to estimate the above-water surface reflectance. Water column properties were then estimated from the above-water reflectance of the mixed spectrum + water column using a semi-analytical optimization model. 4. Estimated water column properties were then applied to the remaining nine spectral endmembers for each benthic class. 5. These nine spectral endmembers from each class + estimated water column were then used to unmix the above-water reflectance in Step 3 using Multiple Endmember Spectral Mixture Analysis (MESMA). The fractional cover of each benthic class estimated by MESMA was then compared to the original, actual fractional cover used to produce the mixed spectrum and fractional cover estimation error was calculated.

ten spectra from each of seven benthic classes, comprised of live brown hermatypic coral, turf algae, crustose coralline algae (CCA), red, brown, and green fleshy algae, and carbonate sand (Fig. 1, Step 1; in-situ reflectance data were obtained from Hochberg et al., 2003). These benthic classes represent common reef benthic classes resolvable by remote sensing technologies and the representative spectra were collected from multiple sites across the global, tropical oceans (Hochberg et al., 2003; Purkis et al., 2019). Spectral mixtures were created as a linear mixture of one coral spectrum, one algal spectrum, and one sand spectrum:

$$\rho = f_{Coral}\rho_{Coral} + f_{Algae}\rho_{Algae} + f_{Sand}\rho_{Sand} \quad (1)$$

where f_i is the fractional cover of each benthic class, ρ_i is the in-situ reflectance spectrum of each benthic class, and i represents either coral, one of the five types of algae, or sand (Fig. 1, Step 1). We used a total of 48 different fractional combinations, which included pure benthic endmembers (Fig. 2). Since only one of the ten endmembers from each class was used to create a spectral mixture, we repeated this process ten times, with each iteration using a different endmember spectrum for each benthic class, for a total of 480 unique spectral mixtures. These mixed spectra were then resampled to AVIRIS spectral bands using known band centers and full width half maximum values (http://aviris.jpl.nasa.gov).

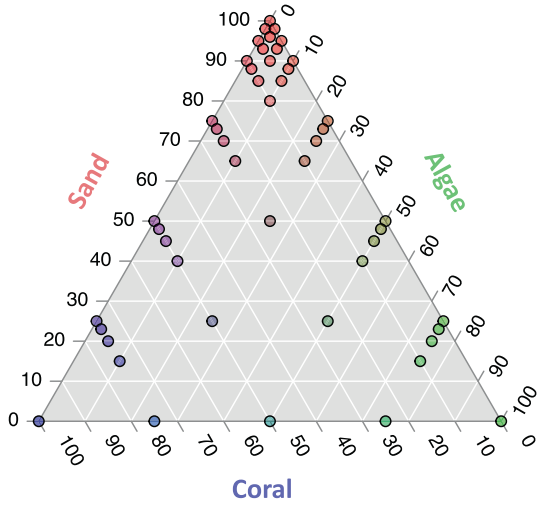

Fig. 2. The 48 fractional mixtures of Coral, Algae, and Sand used in this study. The mixtures include pure (100%) cover types.

2.3. Modeling of diverse water columns

We used the HydroLight radiative transfer model (Version 5.1, Sequoia Scientific) to produce 7000 simulated water columns that represent realistic combinations of seawater chlorophyll concentration, absorption due to colored dissolved organic matter at 440 nm (CDOM), suspended carbonate sediment concentration, surface wind stress, and depth for coral reef systems (Table 1; Hydrolight Case 2 defaults). As the effects of a variable atmosphere were not the focus of this study, the Moderate Resolution Atmospheric Transmission Model (MODTRAN5, Spectral Sciences Inc.) was used to estimate the exoatmosphere downwelling irradiance and was included as an input to the HydroLight models. This downwelling irradiance was then used by HydroLight to convert in-air water-leaving radiance to top of atmosphere remote sensing reflectance. The top of atmosphere remote sensing reflectance was obtained for contiguous spectral bands (~10 nm) which approximate those used by AVIRIS (390–820 nm) over five different bottoms, each of a uniform albedo: 0, 0.25, 0.5, 0.75, 1. Spectral reflectance was interpolated between these five bottom albedo values, at each spectral band, using a piecewise cubic spline to produce reflectance look-up tables as a function of wavelength, similar to methods used in Okin and Gu (2015). Mixed coral reef spectra were then projected through each water column to simulate the top of atmosphere remote sensing reflectance as viewed from above the water surface (Fig. 1, Step 2).

Table 1
The five water column properties (depth, wind speed, colored dissolved organic matter {CDOM}, chlorophyll concentration, and suspended carbonate sediment concentration), values of each property used to simulate the 7000 fully factorial water columns, and references attesting to these values representing the range typically found in tropical coastal waters.

Variable	Values	References
Depth (m)	1, 2, 3, 5, 8, 10, 15	Kleypas et al., 1999; Hochberg et al., 2003
Wind speed (m s^{-1})	0, 1, 2, 5, 10	Phinn et al., 2005
CDOM (m^{-1} at 440 nm)	0.01, 0.02, 0.05, 0.1, 0.5	Siegel et al., 2002, Russell et al., 2019
Chlorophyll concentration (mg m^{-3})	0, 0.1, 0.25, 0.5, 1	Coles and Ruddy, 1995; Mobley et al., 2005; Cooper et al., 2007
Suspended carbonate sediment (g m^{-3})	0, 0.1, 0.25, 0.5, 1, 2, 5, 10	Rogers, 1990; Ogston et al., 2004; Cooper et al., 2007

2.4. Estimation of water column properties

We used a semi-analytical optimization model to estimate the relevant water properties from the simulated remote sensing reflectance of these simulated benthic mixtures projected through the modeled water columns (Fig. 1, Step 3). This approach builds many reflectance spectra from a set of absorption, backscatter, bottom albedo, and water depth values and then uses a bound constrained optimization function (Matlab function 'fminsearchbnd'; lower bounds for all parameters were set to zero and upper bounds left unconstrained) to minimize the difference between it and the measured reflectance spectrum (Lee et al., 1999). The semi-analytical model was then used to retrieve the absorption, backscatter, and water depth of the overlying water column associated with the simulated, above-water reflectance spectra. Chlorophyll and sediment concentrations and absorption due to CDOM, were determined from the estimated absorbance and scattering values which were then used to find the most similar water column (of the 7000 water columns described in Section 2.3) modeled with the HydroLight software (Fig. 1, Step 3; Version 5.1, Sequoia Scientific). To quantify the accuracy of the optimization model we compared the depths estimated from the above-water reflectance spectra to known depths used to build the simulated remote sensing reflectance, a common method to determine the overall efficacy of the model and the accuracy of the estimated water properties (Lee et al., 1999; Stumpf et al., 2003; Thompson et al., 2017).

2.5. Spectral unmixing

The coral reef spectral mixtures projected through the modeled water columns were then unmixed using MESMA to estimate the fractional cover of each benthic class. The MESMA process operates in a similar manner to SMA in that a reflectance spectrum is linearly unmixed using two or more spectral endmembers. However, MESMA is actually many SMAs performed with a series of unique endmember combinations, with one endmember chosen from many for each benthic class (Roberts et al., 1998). The best fit coefficients for each SMA model are calculated and used to construct a modeled reflectance spectrum following Eq. (1). The best model is chosen based on minimizing the root mean squared error between the actual and modeled spectrum. In order to examine the potential reduction in error as more endmembers are utilized, we unmixed the modeled above-water benthic mixture spectra using one to nine unique, randomly selected endmembers for each benthic class.

For each simulated coral reef spectrum projected through a modeled water column, the nine remaining endmembers of each of the three benthic classes were used by MESMA to estimate the fractional cover. Therefore, we used different spectra for the simulation and retrieval steps, as an investigator would never have perfect knowledge of the real endmember spectra when unmixing a hyperspectral image pixel. The summed fractional cover estimates of the three benthic classes were constrained to equal one, with the coral and algal classes equaling the proportional cover of the remaining benthic fraction after the sand cover has been subtracted:

$$f_{Sand_c} = f_{Sand} \tag{2}$$

$$f_{Coral_c} = \frac{|f_{Coral}|}{|f_{Coral}| + |f_{Algae}|}(1 - f_{Sand}) \tag{3}$$

$$f_{Algae_c} = \frac{|f_{Algae}|}{|f_{Coral}| + |f_{Algae}|}(1 - f_{Sand}) \tag{4}$$

where f_{Sand}, f_{Coral}, and f_{Algae} represent the benthic cover fractions derived from MESMA and f_{Sand_c}, f_{Coral_c}, and f_{Algae_c} represent the adjusted benthic fractions after constraining the sum of all benthic cover fractions to one. These adjusted benthic fraction estimates were used for all error calculations.

In order to separate the effect of the water column properties from the effect of the water column estimation scheme on benthic class fractional error, spectral endmembers were also projected through modeled water columns with perfect knowledge of water properties and fractional cover was estimated using the methods described previously.

In addition to calculating fractional cover for each of the 7000 water columns individually, we also examined fractional cover estimated from generalized 'clear' and 'turbid' water conditions. The 'clear' water columns represented all columns where chlorophyll concentration $\leq$ 0.1 mg m^{-3}, sediment concentration $\leq$ 0.1 g m^{-3}, wind speed $\leq$ 5 m s^{-1}, CDOM $\leq$ 0.05 m^{-1}, depth $\leq$ 5 m; and the 'turbid' water column represented all water columns where 0.1 mg m^{-3} $<$ chlorophyll concentration $\leq$ 0.25 mg m^{-3}, 0.1 g m^{-3} $<$ sediment concentration $\leq$ 0.5 g m^{-3}, wind speed $\leq$ 10 m s^{-1}, 0.05 m^{-1} $<$ CDOM $\leq$ 0.1 m^{-1}, depth $\leq$ 5 m. These water columns represent 'clear' and 'turbid' conditions used by Thompson et al. (2017) for coral reef studies where one might expect the feasibility of benthic class discrimination.

The use of spectral derivatives allows for the examination of changes in spectral shape for benthic class separation rather than primarily relying on the magnitude of spectral reflectance (i.e., brightness), which can change dramatically within and across images due to reef structure, depth variability, and illumination conditions (Holden and LeDrew, 1998, 1999; Hochberg and Atkinson, 2000; Hochberg et al., 2003; Catlett and Siegel, 2018). However, the use of spectral derivatives has largely been limited to the identification of specific regions of the spectrum that are most useful for differentiating benthic classes. Here, we apply first and second derivatives to the simulated above-water mixed benthic spectra and above-water endmember spectra in order to exploit differences accentuated by the derivative analysis across the entire spectrum (MATLAB function 'diff'). We then completed the MESMA procedure as detailed above to compare the performance of derivative-based unmixing to native reflectance-based unmixing.

2.6. Error analysis

Several measures of fractional cover error were calculated to examine the effect of water column properties on fractional discrimination accuracy, benthic class separation bias, and the minimum retrievable fraction for each benthic class. The accuracy of benthic

fraction retrieval, or benthic class fractional retrieval error, was determined using the mean absolute error for each benthic fraction (MAE_k), defined as:

$$MAE_{f,k} = \frac{1}{n}\sum_{i=1}^{n} |f_{k,i}^{MESMA} - f_{k,i}^{actual}| \quad (5)$$

where $f_{k,\,i}^{MESMA}$ is the MESMA estimated fractional cover of benthic class k, $f_{k,\,i}^{actual}$ is the original, actual fractional cover of that particular benthic class, and n is the total number of absolute error determinations. Mean absolute error was chosen over root mean squared error because *MAE* is an unambiguous measure of error and is less sensitive to the distribution of error magnitudes (Willmott and Matsuura, 2005).

To quantify bias in fraction retrieval, we determined the mean error for each benthic fraction (ME_k) across the range of different water column properties, which was calculated as:

$$ME_k = \frac{1}{n}\sum_{i=1}^{n} (f_{k,i}^{MESMA} - f_{k,i}^{actual}) \quad (6)$$

Since coral and algae both contain photosynthetic pigments and are spectrally similar, they are often confused for one another in spectral mixture analysis (Hochberg and Atkinson, 2003). We quantified this confusion as the difference between the ME_f of the two benthic classes for all coral and algae combinations where sand was not included in the spectral mixture, calculated as:

$$ME_{Diff} = ME_{Coral} - ME_{Algae} \quad (7)$$

where ME_{Diff} is the bias towards coral being confused for algae. The significance of this difference in *ME* was tested across all algal types using simple linear correlations. In cases where *MAE* or *ME* was > 1 (or < -1) the error level was set equal to 1 (-1).

The cover of benthic classes that comprise coral reef systems can vary considerably across space and various cover types may only represent a small fraction of the measured area of a remote sensing pixel. In order to estimate the minimum fractional cover of each benthic class necessary for spectral discrimination, we quantified the mean relative error (MRE_k), which was calculated as:

$$MRE_k = \frac{1}{n}\sum_{i=1}^{n} \frac{|f_i^{MESMA} - f_i^{actual}|}{f_i^{actual}} \quad (8)$$

When MRE_k is > 1, the fractional cover retrieval error exceeds the total amount of that particular benthic class in the mixture. The point where MRE_k is equal to one represents the minimum fraction where there can be any confidence in benthic class retrieval.

2.7. Validation with in-situ data and aerial hyperspectral imagery

To understand the implications of the simulation analysis for actual hyperspectral imagery, we produced maps of benthic class fractional retrieval uncertainty based on the estimated water column properties of a hyperspectral image acquired over the island of Molokai, Hawaii. Since the benthic fractional cover of this reef is unknown, we use the term 'uncertainty' instead of 'error' for all analyses using the hyperspectral imagery. The southern edge of Molokai is fringed with a wide coral reef, including a shallow reef flat (≤ 2 m depth) dominated by coarse and fine grained eroded sediment which extends ~1 km from shore to an offshore sloping reef (3–30 m depth) characterized by clearer water, calcareous sand, and relatively high coral cover (Storlazzi et al., 2004; Ogston et al., 2004). The hyperspectral image was acquired by the AVIRIS sensor aboard the ER2 High Altitude Airborne Science aircraft as part of the National Aeronautics and Space Administration's Hyperspectral Infrared Imager (HyspIRI) Preparatory Airborne Campaign on January 27, 2017. The data were provided as orthorectified, Level 2 surface reflectance after atmospheric correction based on the Atmosphere Removal Algorithm (ATREM), scattering effect correction with the 6S algorithm, and an empirical correction using in-situ invariant targets (Gao et al., 1993; Vermote et al., 1997; Thompson et al., 2015). In order to correct location errors in the imagery, the AVIRIS image was georeferenced to a pansharpened Landsat 8 Operation Land Imager image of Molokai, Hawaii. Depths > 20 m were masked using the University of Hawaii at Manoa SOEST 50 m multibeam bathymetry product (http://www.soest.hawaii.edu/hmrg/multibeam/bathymetry.php), as were areas with high near infrared (NIR) reflectance indicating land or intertidal areas ($> 3\%$ NIR reflectance).

We used the hyperspectral reflectance data from the AVIRIS image to produce maps of estimated water column properties using the semi-analytical optimization model described previously (Lee et al., 1999). The estimates of water column properties were validated in two ways: 1. Estimates of water column depth were compared against known depths using the SOEST bathymetry product, 2. AVIRIS reflectance was compared to in-situ benthic reflectance after it was projected through the estimated water columns at two sites. Benthic reflectance spectra were collected on Feb 22–23, 2017 across two 20 m transects separated from each other by at least 20 m at each site using a spectrometer mounted inside an underwater housing (1 nm spectral resolution, 325–1075 nm spectral range, ASD Handheld 2, Malvern Panalytical; Hochberg et al., 2003). The mean of ten reflectance spectra, acquired 30 cm off the bottom, every two meters along each transect, were then averaged to produce a mean reflectance spectrum for each transect and then resampled to AVIRIS spectral bands. All spectra were calibrated using a 99% Spectralon panel which was fixed 30 cm from the spectrometer. Both the AVIRIS reflectance and measured reflectance projected through the estimated water columns were smoothed using a Savitsky-Golay filter with a three-band window (Savitsky and Golay, 1964; Hochberg et al., 2003).

We then produced maps of predicted fractional retrieval uncertainty across the reef flat and fore reef of Molokai using the maps of estimated water column properties generated by the semi-analytical inversion model. We matched these estimated water column properties to their closest Hydrolight generated water column to determine that pixel's mean absolute uncertainty for each benthic class based on the simulation analysis.

3. Results

3.1. Effect of water column properties on the estimation of water columns

Accurate estimation of greater depths was compromised with increasing concentrations of chlorophyll and sediment, while increasing wind speed and CDOM had little effect on depth retrieval over the ranges used in this study (Fig. 3; S1–5). The greatest depths (15 m) showed increased error in retrieval at sediment concentrations of 0.2–0.5 g m^{-3}, while concentrations of 1 g m^{-3} and above limited accurate depth retrieval to < 5 m. Estimation of 15 m depths was not severely compromised up to a chlorophyll concentration of 0.5 mg m^{-3}, while concentrations of 1 mg m^{-3} limited accurate depth retrieval to ≤ 5 m.

The estimation of water properties using the optimization methods generally increased error in benthic class fractional cover retrieval compared using the actual 'known' water column properties. Across all spectral derivative analyses and algal types, the estimation process increased the average *MAE* by 0.03 for the 'clear' water columns and by 0.16 for the 'turbid' water columns versus having perfect knowledge of the water column properties. This shows that the optimization scheme is less accurate in estimating water column properties in turbid conditions but performs well under relatively clear water conditions, using mixtures containing turf algae as an example (Fig. 4; Table S1). Since water column properties are rarely known when analyzing remotely sensed imagery, all subsequent analyses were performed using water columns with properties estimated by the semi-analytical optimization model, unless stated otherwise.

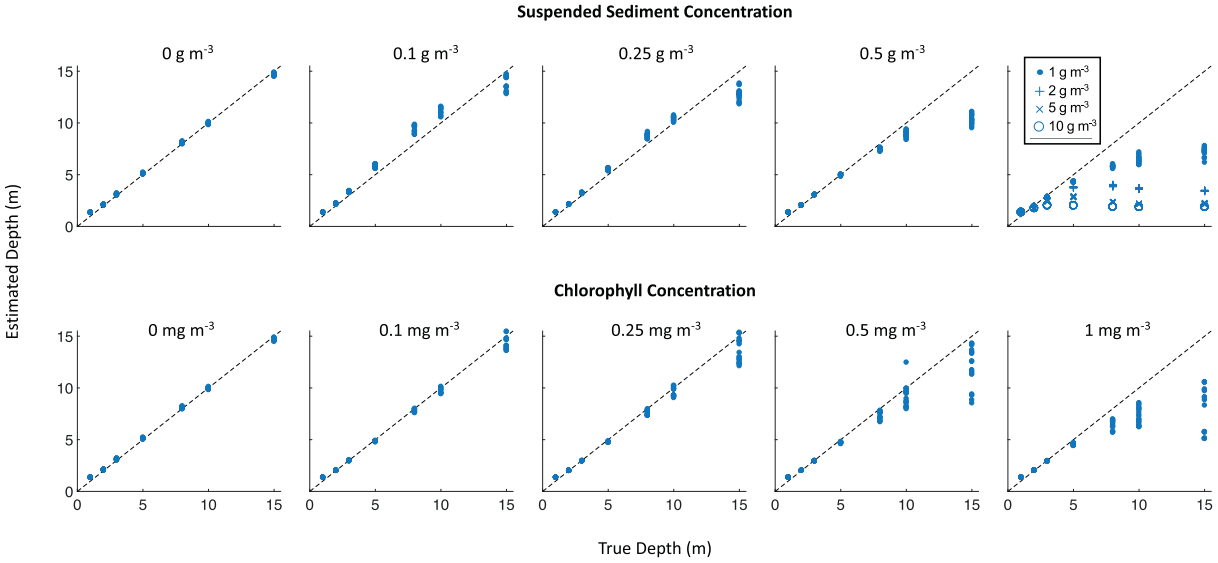

Fig. 3. Water column depth estimated by the semi-analytical optimization model compared against known (True) depth across the range of suspended sediment and chlorophyll concentrations used in this study. These relationships were derived from spectra containing mixtures of Coral, Turf Algae, and Sand. The dashed black line represents the 1:1 line.

3.2. Effect of MESMA on fraction retrieval error

Increasing spectral endmembers used for unmixing generally decreased error in fractional cover retrieval for both native spectra and spectral derivative analyses. For example, using the first derivative of the reflectance spectra and water columns estimated by the semi-analytical optimization model, increasing the number of spectral endmembers from one to nine decreased the mean absolute error by 9% for coral (*MAE* decreased from 0.154 to 0.140), 19% for turf algae (*MAE* decreased from 0.186 to 0.151) and by 10% for sand (*MAE* decreased from 0.161 to 0.145) across all 'clear' water cases at depths ≤5 m, however the magnitude of this effect varied across algal types (Fig. 5; S6–9). In light of the improvements observed by using nine spectral endmembers for each class, these results were used for the subsequent analyses.

3.3. Use of spectral derivatives to retrieve benthic class fractional cover

In order to determine whether the use of spectral derivatives improved the accuracy of benthic class fractional retrieval, we determined the error when first or second derivatives of endmember reflectance spectra before unmixing. The first derivative of reflectance presented the lowest average *MAE* for both 'clear' and 'turbid' water columns and similar *ME* to native reflectance, without the amplification of *ME* observed for 'turbid' water columns using the second derivative analysis (Fig. 4; Table S1). Due to this reduction in *MAE*, the first derivative of reflectance was used for all subsequent analyses.

3.4. Effect of water column properties on benthic class fraction retrieval

We determined the benthic class fractional cover retrieval error across 7000 water columns which allowed for the examination of error

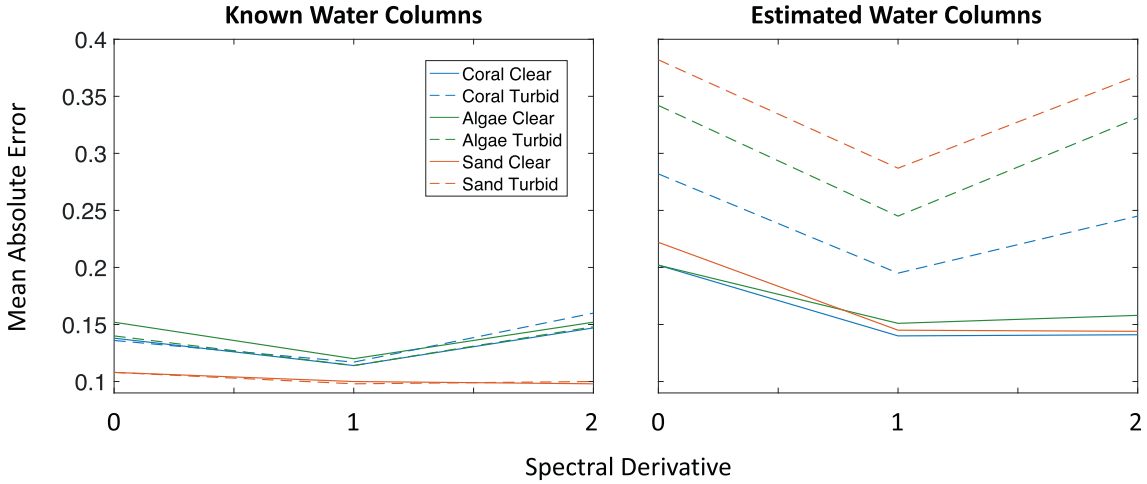

Fig. 4. The mean absolute error in fractional cover retrieval for each benthic class (Coral, Turf Algae, Sand) combination using spectral derivative analysis. Error was calculated using both 'known water columns' where there was perfect knowledge of water column properties, and 'estimated water columns', where water column properties were estimated by the semi-analytical optimization model. Errors reported represent the average of all mean absolute errors under 'clear water' (solid lines; chlorophyll concentration ≤ 0.1 mg m^{-3}, sediment concentration ≤ 0.1 g m^{-3}, wind speed ≤ 5 m s^{-1}, CDOM ≤ 0.05 m^{-1}, depth ≤ 5 m) and 'turbid water' (dashed lines; 0.1 < chlorophyll concentration ≤ 0.25 mg m^{-3}, 0.1 g m^{-3} < sediment concentration ≤ 0.5 g m^{-3}, wind speed ≤ 10 m s^{-1}, 0.05 m^{-1} < CDOM ≤ 0.1 m^{-1}, depth ≤ 5 m) conditions.

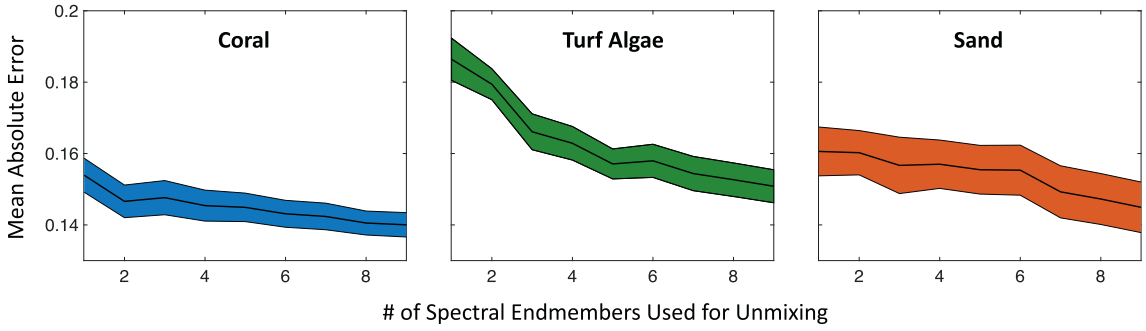

Fig. 5. Change in the mean absolute error for each benthic class as the number of the spectral endmembers used in the Multiple Endmember Spectral Mixture Analysis (MESMA) process is increased from 1 to 9 spectral endmembers for each class. Errors reported represent the average of all mean absolute errors under 'clear water' conditions at a depth of ≤5 m. Shaded area shows the standard error.

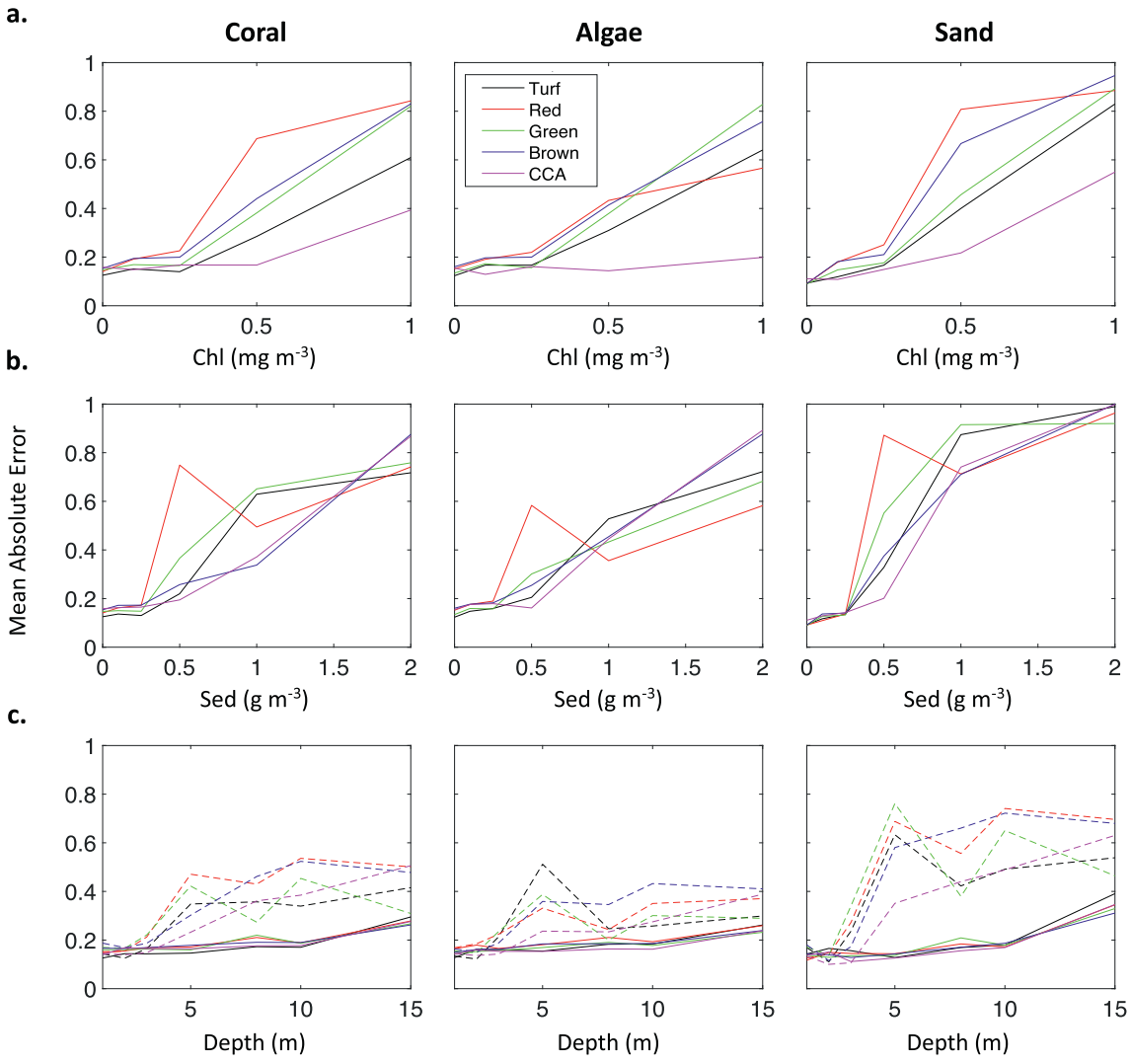

Fig. 6. Change in the mean absolute error of the three benthic classes as a) chlorophyll concentration, b) suspended sediment concentration, and c) depth is increased. The different colored lines represent mixtures which contain one of five different algal types. In the first two rows, depth is held constant at 5 m. In the bottom row, the solid lines represent 'clear' and the dashed lines represent 'turbid' water conditions.

over the range of water properties investigated here (Table 1). Given the large number of water column property combinations included in this study and because chlorophyll, sediment concentration and depth contributed the most to fractional cover retrieval error, only a few cases were examined in detail (Fig. S10). To examine the impact of water column chlorophyll concentration, we used cases with sediment concentration = 0 g m^{-3}, CDOM ≤ 0.05 m^{-1}, wind speed ≤ 5 m s^{-1}, and depth = 5 m. While there were differences in *MAE* across algal types, error did not increase dramatically for coral, algae, and sand until chlorophyll concentrations were ≥0.5 mg m^{-3} (Fig. 6a). To examine how error changed over a range of sediment concentrations, we used cases with chlorophyll concentration = 0 mg m^{-3},

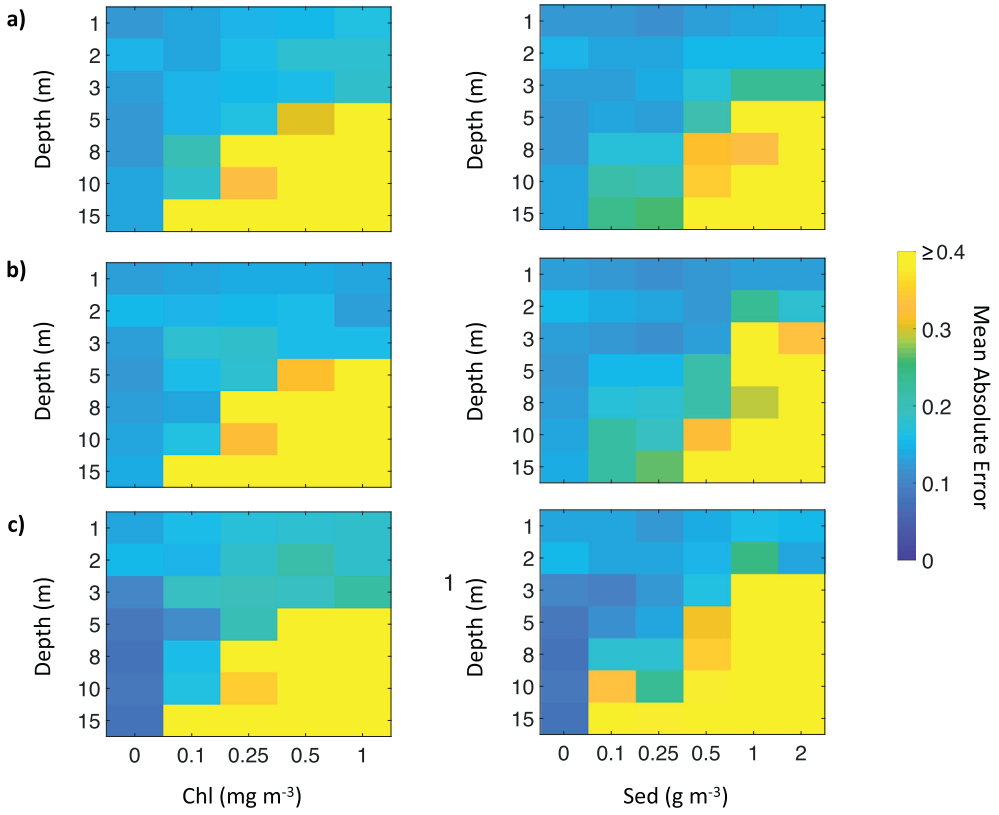

Fig. 7. Bivariate plots showing the mean absolute error for a) Coral, b) Turf Algae, and c) Sand as a function of chlorophyll concentration versus depth and suspended sediment concentration versus depth.

CDOM $\leq$ 0.05 m^{-1}, wind speed $\leq$ 5 m s^{-1}, and depth = 5 m. We found that there was a precipitous increase in *MAE* for coral, algae, and sand at sediment concentrations > 0.2 mg m^{-3}, and that this increase was especially sudden for *MAE* associated with sand and when the mixed spectra contained red algae (Fig. 6b). Changes in error due to depth were investigated using the 'clear' and 'turbid' water definitions described above. While increases in *MAE* were modest for coral, algae, and sand across all depths, there was an increase in *MAE* for depths > 3 m for the 'turbid' water columns, especially for sand (Fig. 6c).

Bivariate combinations of water properties indicated some combinative effects (Fig. 7). *MAE* remains relatively low for all depths when chlorophyll concentration = 0 mg m^{-3} (sediment concentration = 0 g m^{-3}, CDOM $\leq$ 0.5 m^{-1}, wind $\leq$ 10 m s^{-1}), and then increases rapidly at depths $\geq$5 m when chlorophyll concentration is $\geq$0.25 mg m^{-3} for coral, algae, and sand benthic classes (Fig. 7). Combinations of sediment concentration and depth showed that sediment concentrations $\geq$0.5 g m^{-3} dramatically increased *MAE* of benthic cover fractional retrieval at depths > 5 m. This was especially true for the sand benthic class, where even low levels of sediment $\geq$0.1 g m^{-3} increased the *MAE* to relatively high levels at depths $\geq$10 m (Fig. 7). The bivariate effects on *MAE* for combinations of chlorophyll and sediment concentrations show a relative narrow window where low error was achieved. If chlorophyll and sediment concentrations were both > 0.1 mg m^{-3} and 0.1 g m^{-3} respectively, high *MAE* can be anticipated for all benthic classes at depths $\geq$5 m (Fig. 8). Additional figures for each algal type and effects of bivariate combinations of chlorophyll and sediment concentrations at different depths can be found in the supplement (Figs. S11–18).

3.5. Effect of water column properties on benthic class confusion

Differences in *ME* were used to examine the effect of water properties on the confusion between coral and algae fractional retrieval error. As depth increased there was a consistent bias towards confusing coral for algae (chlorophyll concentration = 0 mg m^{-3}, sediment concentration = 0 g m^{-3}, CDOM = 0.01 m^{-1}, wind = 0 m s^{-1}; Fig. 9). Across all algal types, this effect was significant with $r = -0.59$ and $p < 0.01$ (here and elsewhere, 'r' is the Pearson correlation coefficient). As chlorophyll concentration increased, there was significantly more algae being confused for coral with $r = 0.56$ and $p < 0.01$ (sediment concentration = 0 g m^{-3}, CDOM = 0.01 m^{-1}, wind = 0 m s^{-1}, depth = 5 m; Fig. 9), although this effect was variable across depths (Fig. S19). As sediment concentration increased there was variability in bias across algal types. Both red and green algae were more often confused for coral as sediment concentration increased, however there was no overall significant effect across all algal types ($r = 0.31$, $p = 0.094$; chlorophyll concentration = 0 mg m^{-3}, CDOM = 0.01 m^{-1}, wind = 0 m s^{-1}, depth = 5 m; Fig. 9).

3.6. Minimum benthic class fractions necessary for discrimination

The minimum fractional cover necessary for retrieval was assessed by using the *MRE*. All minimum fractional cover estimates were assessed under 'clear' water conditions. Coral minimum fraction cover reached *MRE* equal to one at 0.1 fractional cover with a decrease to *MRE* equal to 0.5 at a fractional cover of 0.25 (Fig. 10). Minimum fractional cover for turf algae reached *MRE* equal to one at 0.12 fractional cover with a decrease to *MRE* equal to 0.5 at a fractional cover of 0.25 (Fig. 10; S20–23) and sand fractional cover *MRE* remained under one for all investigated benthic cover fractions (minimum fractional cover used = 0.15; Fig. 10). Extrapolation of the sand minimum fractional cover reached the *MRE* equal to 1 threshold at 0.05 cover.

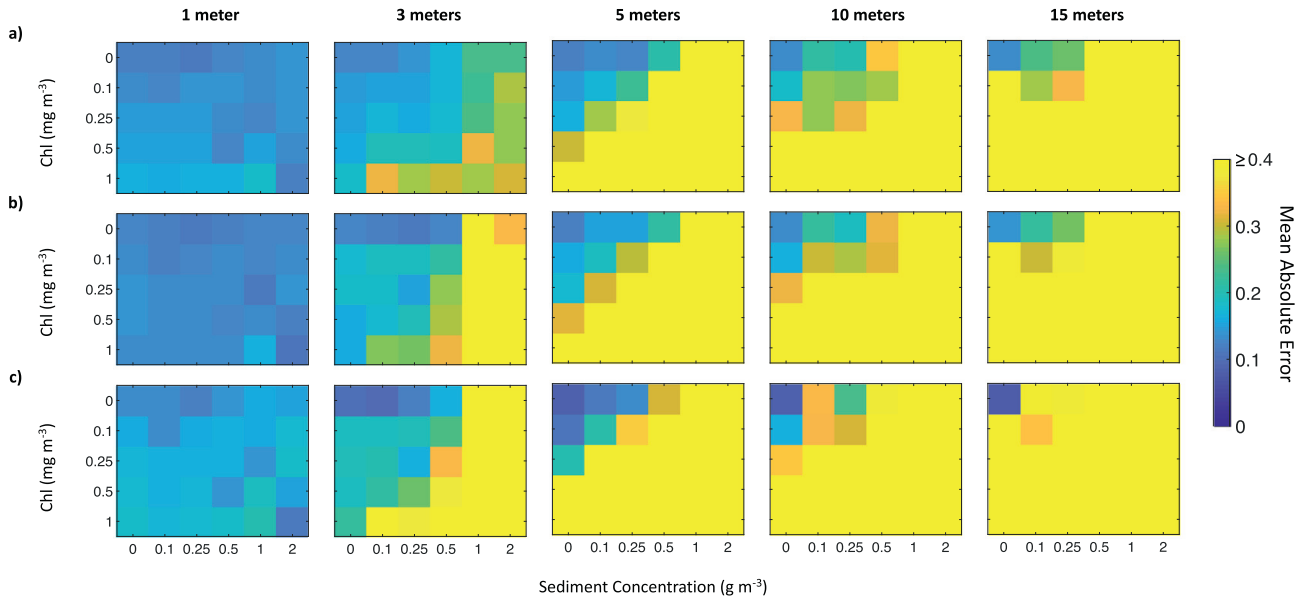

Fig. 8. Bivariate plots showing the mean absolute error for a) Coral, b) Turf Algae, and c) Sand as a function of chlorophyll concentration versus suspended sediment concentration across different water column depths.

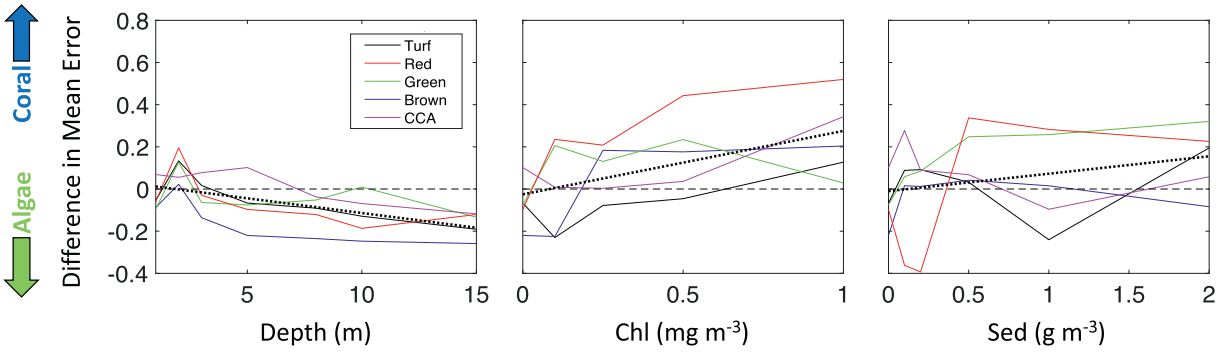

Fig. 9. The difference in mean error between the Coral and Algae benthic classes as a function of depth, chlorophyll concentration, and suspended sediment concentration. Positive differences in mean error represent a bias towards Coral and negative differences show a bias towards Algae. The different colored solid lines show different algal types and the dotted black line shows the mean relationship across the different algal types.

3.7. Application of simulation analysis to hyperspectral imagery

The semi-analytical optimization model estimated high concentrations of suspended sediment and chlorophyll and high absorption due to CDOM on the shallow reef flat nearshore of Molokai, while deeper areas offshore of the reef crest displayed much lower levels of these water column constituents (Fig. 11). Estimated water column depth was closely related to known depth from 0 to 10 m, while depth was increasingly underestimated by the model from 11 to 20 m (r^2 = 0.86, $p < 0.001$; Fig. 11). Removing the pixels with estimated 'turbid' water properties decreased the scatter but did not change the overall relationship (r^2 = 0.87, $p < 0.001$; Fig. 11). The measured benthic reflectance projected through the estimated water columns compared well to the AVIRIS reflectance in both magnitude and shape (Fig. 12).

Since the validation steps showed satisfactory results, we generated maps of predicated absolute uncertainty for each benthic class across

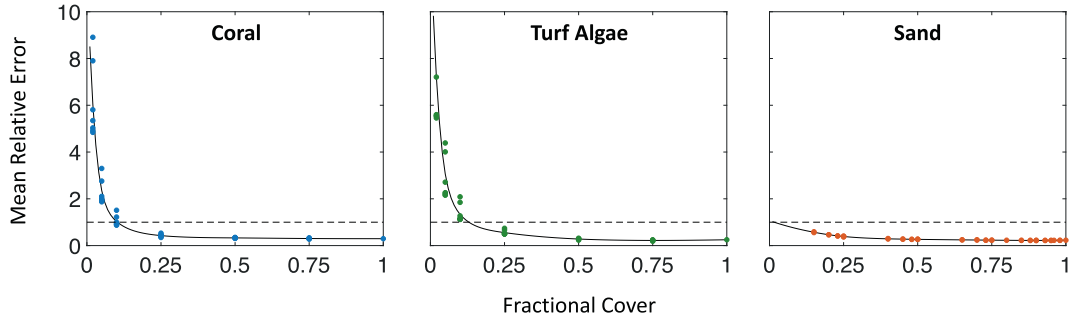

Fig. 10. The mean relative error for the three benthic classes as a function of the known fractional cover of each class. The solid black line shows the best fit line and the dashed black line shows where the mean relative error equals 1, the point where the amount for fractional retrieval error equals the fraction of the class present in the mixture. This analysis was performed under 'clear water' conditions at a depth of 5 m.

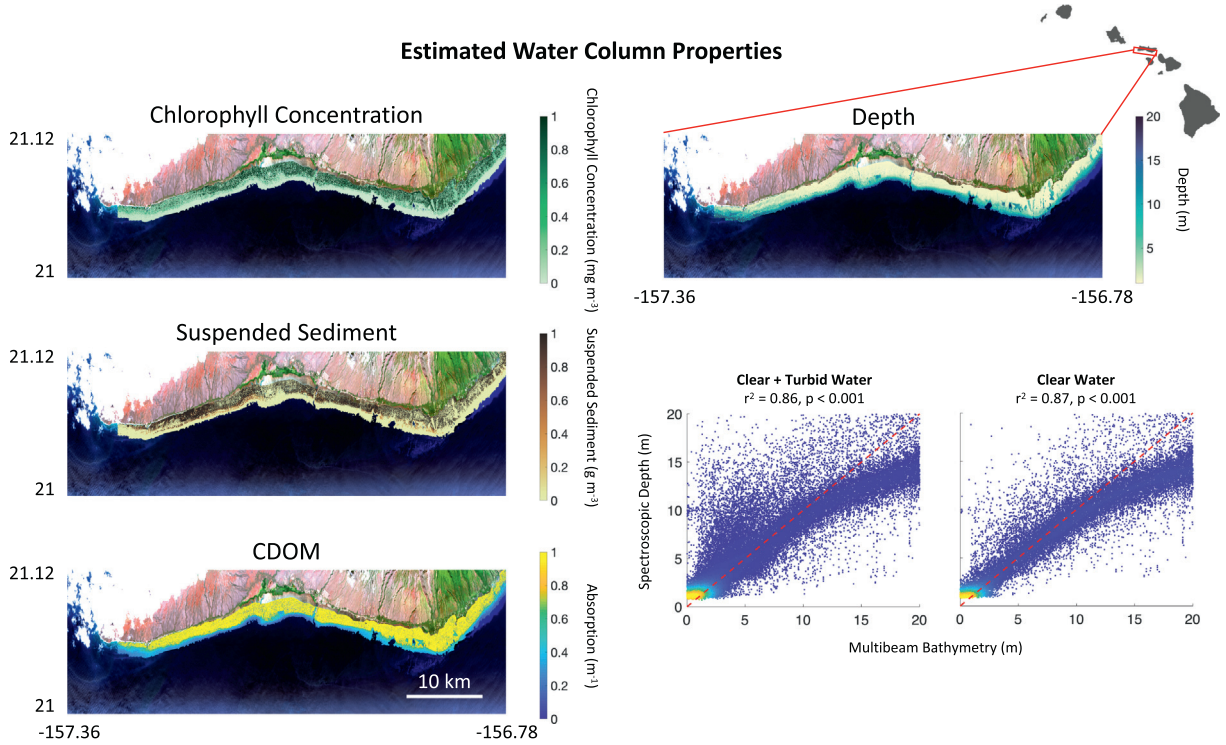

Fig. 11. Water property values estimated by the semi-analytical optimization model from the January 27th, 2017 AVIRIS image of the southern side of Molokai. Spectroscopic depth estimated from the imagery were compared with known bathymetry from multibeam sonar under all water conditions and clear water conditions (suspended sediment concentration < 0.1 g m^{-3} and chlorophyll concentration < 0.1 mg m^{-3}).

the coral reef system (Fig. 13). The shallow reef flat, which was estimated to have high levels of light absorbing and scattering water constituents generally showed high levels of uncertainty for all benthic classes. Uncertainty decreased in areas offshore of the reef crest, where depth increased and water column constituent concentrations were decreased. The uncertainty associated with the fractional retrieval of coral cover was consistently low in these deeper, clearer waters while the uncertainty for turf algae cover was generally higher than for coral cover but decreased as distance from the reef flat increased. Fractional retrieval uncertainty for sand cover was lower than coral and turf algae and decreased to an absolute uncertainty of < 0.1 just offshore of the reef crest before marginally increasing in deeper waters.

4. Discussion

4.1. Using MESMA to estimate fractional cover of spectrally variable benthic classes

Due to the spatial scale of most spaceborne sensor pixels, assessing subpixel fractional cover of coral, algae, and sand is paramount to quantifying change though time and understanding the effects of human and environmental stressors (Hochberg and Atkinson, 2003; Hedley et al., 2004). Producing accurate fractional cover estimates of common coral reef benthic classes from reflectance is dependent on the selection of representative endmember spectra (Dennison and Roberts, 2003). The use of a single representative spectral endmember for each benthic class may lead to increased retrieval error or a misinterpretation of the existing benthic types (Fig. 5). Different taxa of algae vary spectrally due to their varying types and proportions of pigments (Kirk,

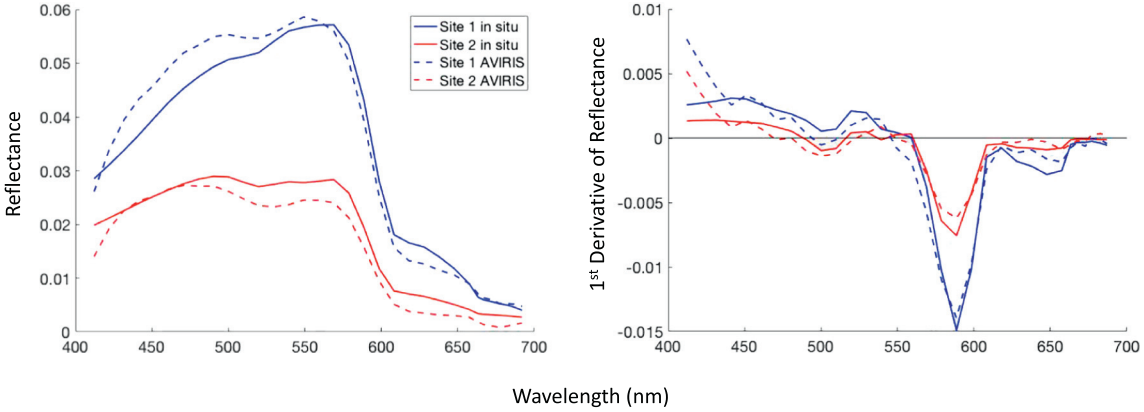

Fig. 12. Comparison of remotely sensed (AVIRIS; dashed lines) and in-situ benthic reflectance projected through water columns estimated using the semi-empirical optimization model (solid lines). The plot on the left shows the native reflectance spectra and plot on the right shows the first derivative of the spectra.

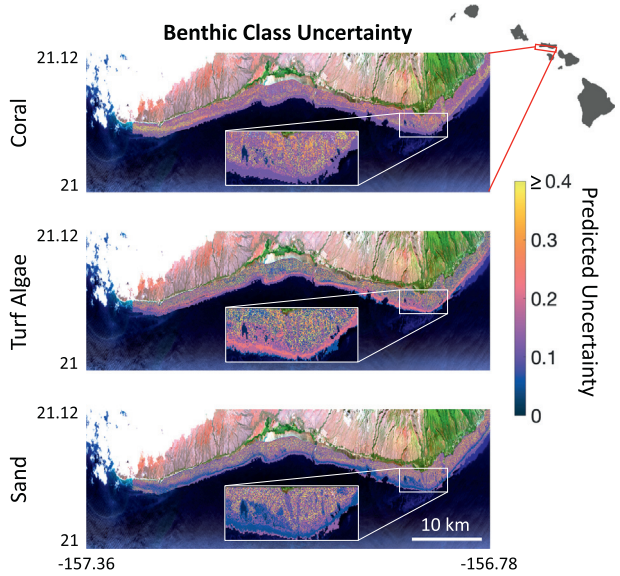

Fig. 13. Maps of predicted uncertainty for each benthic class are shown following the results obtained from the simulation analysis presented in this study for the January 27th, 2017 AVIRIS image of the southern side of Molokai. Predicted uncertainty was derived for each 18 m pixel from the water property values estimated by the semi-analytical optimization model.

1994; Hochberg et al., 2003). Choosing a single algal type, or the average spectrum of multiple algal types, in a spectral mixing model leads to uncertainty in the accuracy of the fractional retrievals (Fig. 6). Once the magnitude of reflectance is normalized, the spectral shape of coral is fairly conserved across taxonomic and geographic space (Hochberg et al., 2004). However, the decrease in fractional retrieval error as the number of coral, algae, and sand endmembers are increased is evidence that it may be important to account for these subtle differences in spectral shape for coral reef systems as well (Fig. 5).

The distinctive spectral shapes of reflectance for the coral and algal benthic classes is the result of varying photosynthetic and photoprotective pigments (such as peridinin, which is present in the symbiotic dinoflagellates in coral), however the concentrations and ratios of these pigments change through time due to both extrinsic and intrinsic factors. For example, pigment concentrations or density of the symbiotic zooxanthellae in coral polyps may vary with changes in light, temperature, disease, or the genetic diversity of the symbionts themselves (Kinzie et al., 1984; Anderson et al., 2013; Torres-Pérez et al., 2015; Russell et al., 2016). Changes in algal pigments can occur in response to changes in ambient nutrient or light conditions but may also be an indicator of age or senescence processes (Louda et al., 1998; Bell et al., 2018; Bell & Siegel, in review). Variations in pigment concentrations can affect the magnitude of differences between different parts of the reflectance spectrum and thus the spectral slope (Bell et al., 2015). One can capitalize on these changes in spectral slope by using derivative analysis for spectral unmixing. Using the first derivative of the simulated mixed spectrum and spectral endmembers decreased the mean absolute error of benthic class retrieval relative to the native spectra and second derivatives across 'clear' and 'turbid' water conditions. Combining spectral derivative analysis with the use of multiple spectral endmembers could be used to simultaneously accentuate these subtle changes in spectral slope for discrimination between benthic classes and account for spectral variability due to physiological condition within a benthic class.

4.2. Effect of water column properties on benthic fractional discrimination error

The fully crossed set of modeled water columns used in this study allows water properties to be held constant to isolate the effect that an individual water constituent has on the fractional cover retrieval error. It is encouraging that both chlorophyll and sediment concentrations lead to relatively low fractional retrieval error over the ranges often found in coastal tropical waters (i.e. 0–0.25 mg m^{-3} chlorophyll, 0–0.25 g m^{-3} sediment; Mobley et al., 2005; Cooper et al., 2007). However, there are notable differences in fractional retrieval error as a function of benthic class and water property (Fig. 6). For example, as water column sediment concentration increases, the fractional retrieval error of sand rises more dramatically than both coral and algae (Ackleson et al., 2018). This is not surprising as suspended carbonate sediment has spectral qualities similar to those of benthic sand and also prevents light reflected by coral and algae from leaving the water column (Stephens et al., 2003; Dierssen et al., 2009). Additionally, the type of algae present in the mixed spectrum can affect the fractional retrieval error of coral and sand. Mixed spectra containing red macroalgae often display increased fractional retrieval error for all benthic classes as chlorophyll and sediment concentrations increase, relative to spectral mixtures containing other algal types (Fig. 6). However, the opposite effect is observed for mixed spectra containing crustose coralline algae (CCA), where fractional retrieval error remains relatively low as water column chlorophyll concentration increases. Macroalgae are a natural component of a coral reef system, although the abundance and composition of these species may be indicative of reef degradation (Hughes, 1994; Jompa and McCook, 2003). Conversely, CCA is generally considered beneficial and may suppress macroalgal growth and recruitment (Vermeij et al., 2011). The diverging trends in error between these different types of algae, in concert with their opposing ecological effects, argues for a conservative approach (i.e., a lower allowable concentration of water properties such as chlorophyll and sediment concentrations) when analyzing remotely sensed imagery.

In reality, the spectral effects of these water properties never exist in isolation. For example, the effects of chlorophyll concentration are also a function of water column depth. Therefore, it is useful to examine the bivariate effects of water properties to determine best practices for the fractional cover retrieval of natural coral reef systems. While it is possible to accurately unmix coral reef spectra at 15 m depth, low fractional cover retrieval errors only exist when both chlorophyll and sediment concentrations are equal to zero (Figs. 7 & 8). Generally, if chlorophyll concentration is > 0.1 mg m^{-3} and sediment concentration is > 0.1 g m^{-3}, then only depths < 5 m should be classified, while coral reef spectra can be unmixed under most water conditions at depths of ≤ 3 m (Fig. 8).

Additionally, because we can calculate how water column properties affect fractional retrieval error, it is possible to examine how this error might vary across space using hyperspectral imagery (Fig. 13). The water column properties estimated from the AVIRIS image of Molokai match previous descriptions of the island: a shallow, turbid reef flat due to the deposition of eroded sediments and a sloping fore reef consisting of deeper, clear waters offshore of the reef crest (Storlazzi et al., 2004; Ogston et al., 2004). Most benthic cover estimates on the turbid reef flat would be highly suspect, while areas in the clearer waters of the fore reef should be more accurate and suitable for further analysis. These maps of fractional retrieval uncertainty can help the investigator filter out benthic cover estimates where the uncertainty exceeds a pre-determined threshold or identify specific areas or entire images with poor fractional retrieval accuracy. Knowledge of the fractional cover retrieval uncertainty is essential for any time series analysis of coral reef systems, as the fractional retrieval uncertainty due to variable water conditions could mask significant change in coral reef health.

A spaceborne, repeat hyperspectral measurement approach like the one recommended by the Decadal Survey for Earth Science Application from Space (National Academies of Sciences, Engineering, and Medicine, 2018), will collect repeat imagery of the world's coral reefs, aid in the identification of adverse water conditions (such as high

concentrations of chlorophyll or sediment, or the presence of a phytoplankton type with similar pigments to coral, like dinoflagellates) and decrease uncertainty of fractional cover estimates. The retrieval of water column depths (1–15 m) using semi-analytical optimization methods is accurate under most water conditions that favor low benthic class fractional retrieval error (Figs. 3, 11; Lee et al., 1999). Multiple images of the same area can be used to create a bathymetry map for any shallow reef system. Since water constituents may vary greatly through time, estimated depths which deviate from the long-term mean will serve as additional evidence that the water column properties are not amenable to benthic class fractional cover retrievals. These long-term depth estimates could also be used as strong priors for Bayesian methods used to estimate benthic reflectance spectra (Thompson et al., 2017). Though the benthic community on coral reefs can rapidly change due to disturbance events, invasive species, or environmental conditions which lead to coral bleaching or macroalgal blooms, these events are typically sporadic. Multiple, consecutive images of benthic class stability are common over likely SBG repeat intervals (*proposed* 16 days; Andréfouët et al., 2001; Lee et al., 2015). These instances of similar fractional cover estimates will help decrease uncertainty and serve as a valuable baseline from which to measure change.

4.3. Challenges to the accurate detection and discrimination of benthic cover types

Although the native reflectance spectra of coral and benthic algae can be distinguished from one another, the properties of the overlaying water column may introduce biases by attenuating, obscuring, or altering major reflectance features essential for accurate discrimination (Hochberg and Atkinson, 2000; Hedley et al., 2004). Increases in depth lead to an increase in fractional retrieval confusion where coral cover is biased towards algal cover regardless of the algal type in the spectral mixture (Fig. 9). Many of the major reflectance features indicating differences in spectral shape between coral and algae occur at wavelengths between 520 and 580 nm, a region which is attenuated by seawater over depths common to coral reef systems (Hochberg and Atkinson, 2000). There is also an increase in fractional retrieval confusion where algal cover is biased towards coral cover as water column chlorophyll concentration increases (Fig. 9). While this bias is noteworthy, the rate of increase in fractional retrieval error varies as a function of algal type and is most problematic at water column chlorophyll concentrations above what is recommended for benthic cover fraction retrieval from the results presented in this study.

The minimum fraction of a particular benthic class detectable inside a remote sensing pixel is especially important as coral cover may vary widely and may be dependent on the spatial scale of observation (Rogers and Miller, 2006; Bruno and Selig, 2007; Hedley et al., 2012). Coral and algal cover may have to be $> 25\%$ (under 'clear' water conditions at 5 m depth) in order to be assessed with the accuracy necessary for coral reef monitoring or ecological studies (Fig. 10). However, even these larger thresholds may be of use for the fractional retrieval of fleshy macroalgae. Coral reef systems can be periodically covered by dense mats of macroalgae, although the drivers of these formations are debated (*reviewed in* McCook, 1999; Burkepile and Hay, 2006; Mumby et al., 2013). Assessing the dynamics of macroalgal cover across space may provide needed insight to these questions. A high fractional threshold for coral may already rule out its detection at some locations, especially degraded reef systems (Hughes, 1994). However remote sensing offers the ability to map coral reefs across vast areas. Many contiguous pixels displaying low fractional cover of a particular benthic class increases the confidence of coral reef state compared to the minimum detectable fraction uncertainty of a single pixel.

Coral reefs are more complex and can contain more benthic classes than were investigated in this study. Reefs are three dimensional structures which feature small scale changes in depth inside the area of a typical medium resolution remote sensing pixel. These variations in depth may be correlated with different benthic classes and this complexity should be considered when uncertainty estimates are made. The types of benthic algae, investigated individually here, often occur together over relatively small areas. A natural extension to this work would be test the identification of a dominant algal type using endmembers from all algal types inside the algal endmember library. Another possibility is the estimation of fractional cover of multiple algal types simultaneously and the resulting effects on the fractional retrieval error of other benthic classes from this added spectral complexity. We did not investigate the error related to a variable atmosphere or solar elevation in this study, however previous studies have shown that spectral variation of benthic types and sub-pixel mixing are the dominant drivers of fractional retrieval error and robust atmospheric correction algorithms for hyperspectral imaging of coral reefs are nascent (Hedley et al., 2012; Thompson et al., 2017).

5. Conclusions

We assessed the role of a set of water column properties, over realistic ranges, on the fractional cover retrieval of common coral reef benthic classes. Our results establish 'best practices' for appropriate water conditions for the satisfactory estimation of fractional benthic class cover, where depths of ≥ 5 m should be classified only if chlorophyll and sediment concentration are < 0.1 mg m^{-3} and < 0.1 g m^{-3}, respectively, while fractional cover can be estimated under most water column conditions at depths ≤ 3 m. Furthermore, maps of predicted fractional cover retrieval error generated from hyperspectral imagery will guide the investigator in the use and interpretation of unmixing results. The use of multiple spectral endmembers can reduce benthic fractional retrieval error across all benthic classes. The decreased fractional retrieval error associated with the use of the spectral first derivative during unmixing analysis shows that spectral shape is more important for accurate benthic class fraction retrieval when compared to spectral brightness. The minimum fractional cover of benthic classes, especially coral and algae, needs to be $\geq 25\%$ in order to have a mean relative error $< 50\%$, but these thresholds can still be useful to ecological studies.

Simulation studies are ultimately best-case scenarios which will be sensitive to difficulties in atmospheric and radiometric correction, reef structural complexity, and sensor limitations (Hedley et al., 2012; Thompson et al., 2017). However, with the advent of a global hyperspectral satellite sensor, such as the SBG designated observable, there are many ways to leverage repeat measurements to produce more accurate and useful fractional cover data.

Author contribution statement

TWB, KCC, and GSO conceived the study. TWB and EJH collected and processed the data. TWB led the analysis. TWB wrote the manuscript. All authors contributed to interpreting the results and revising the manuscript.

Declaration of competing interest

The authors declare that they have no known competing financial interests or personal relationships that could have appeared to influence the work reported in this paper.

Acknowledgments

We would like to acknowledge the support of the National Aeronautics and Space Administration through the Hyperspectral Infrared Imager (HyspIRI) Preparatory Airborne Campaign (grant numbers NNX15AT98G and NNX15AR99G) and the NASA Earth Venture Suborbital-2 program for funding the COral Reef Airborne Laboratory (CORAL; grant number NNX16AB05G). We would also like

to extend thanks to Dr. Liane Guild and Dr. Juan Torres-Perez for assistance with underwater spectroscopy training and Dr. Curtis Mobley and Dr. James Allen for assistance with the HydroLight software. Special thanks are given to Dr. Ku'ulei Rodgers for hosting our team at the Hawai'i Institute of Marine Biology. We also would like to thank three reviewers (both anonymous and identified) for their constructive feedback.

Appendix A. Supplementary data

Supplementary data to this article can be found online at https://doi.org/10.1016/j.rse.2019.111631.

References

Ackleson, S., Moses, W., Montes, M., 2018. Remote sensing of coral reefs: uncertainty in the detection of benthic cover, depth, and water constituents imposed by sensor noise. Appl. Sci. 8, 2691. https://doi.org/10.3390/app8122691.

Anderson, D.A., Armstrong, R.A., Weil, E., 2013. Hyperspectral sensing of disease stress in the Caribbean reef-building coral, Orbicella faveolata - perspectives for the field of coral disease monitoring. PLoS One 8, e81478. https://doi.org/10.1371/journal.pone.0081478.

Andréfouët, S., Muller-Karger, F.E., Hochberg, E.J., Hu, C., Carder, K.L., 2001. Change detection in shallow coral reef environments using Landsat 7 ETM+ data. Remote Sens. Environ. 78, 150–162. https://doi.org/10.1016/S0034-4257(01)00256-5.

Andréfouët, S., Berkelmans, R., Odriozola, L., Done, T., Oliver, J., Muller-Karger, F., Andrefouet, S., 2002. Choosing the appropriate spatial resolution for monitoring coral bleaching events using remote sensing. Coral Reefs 21, 147–154. https://doi.org/10.1007/s00338-002-0233-x.

Anthony, K.R.N., Maynard, J.A., Diaz-Pulido, G., Mumby, P.J., Marshall, P.A., Cao, L., Hoegh-Guldberg, O., 2011. Ocean acidification and warming will lower coral reef resilience. Glob. Chang. Biol. 17, 1798–1808. https://doi.org/10.1111/j.1365-2486.2010.02364.x.

Bell, T.W., Siegel, D.A., in review. Nutrient Availability and Senescence Spatially Structure the Dynamics of an Ecosystem Engineer.

Bell, T.W., Cavanaugh, K.C., Siegel, D.A., 2015. Remote monitoring of giant kelp biomass and physiological condition: an evaluation of the potential for the Hyperspectral Infrared Imager (HyspIRI) mission. Remote Sens. Environ. 167, 218–228. https://doi.org/10.1016/j.rse.2015.05.003.

Bell, T.W., Reed, D.C., Nelson, N.B., Siegel, D.A., 2018. Regional patterns of physiological condition determine giant kelp net primary production dynamics. Limnol. Oceanogr. 63, 472–483. https://doi.org/10.1002/lno.10753.

Bruno, J.F., Selig, E.R., 2007. Regional decline of coral cover in the Indo-Pacific: timing, extent, and subregional comparisons. PLoS One 2, e711. https://doi.org/10.1371/journal.pone.0000711.

Burkepile, D.E., Hay, M.E., 2006. Herbivore vs. nutrient control of marine primary producers: context-dependent effects. Ecology 87, 3128–3139.

Catlett, D., Siegel, D.A., 2018. Phytoplankton pigment communities can be modeled using unique relationships with spectral absorption signatures in a dynamic coastal environment. J. Geophys. Res. Oceans 123, 246–264. https://doi.org/10.1002/2017JC013195.

Coles, S.L., Ruddy, L., 1995. Comparison of water quality and reef coral mortality and growth in Southeastern Kane'ohe Bay, O'ahu, Hawai'i, 1990 to 1992, with conditions before sewage diversion. Pac. Sci. 49, 247–265.

Cooper, T.F., Uthicke, S., Humphrey, C., Fabricius, K.E., 2007. Gradients in water column nutrients, sediment parameters, irradiance and coral reef development in the Whitsunday Region, central Great Barrier Reef. Estuar. Coast. Shelf Sci. 74, 458–470. https://doi.org/10.1016/j.ecss.2007.05.020.

Dennison, P.E., Roberts, D.A., 2003. Endmember selection for multiple endmember spectral mixture analysis using endmember average RMSE. Remote Sens. Environ. 87, 123–135. https://doi.org/10.1016/S0034-4257(03)00135-4.

Dierssen, H.M., Zimmerman, R.C., Burdige, D.J., 2009. Optics and remote sensing of Bahamian carbonate sediment whitings and potential relationship to wind-driven Langmuir circulation. Biogeosciences 6, 487–500. https://doi.org/10.5194/bg-6-487-2009.

Dollar, S.J., Tribble, G.W., 1993. Recurrent storm disturbance and recovery: a long-term study of coral communities in Hawaii. Coral Reefs 12, 223–233. https://doi.org/10.1007/BF00334481.

Gao, B.C., Heidebrecht, K.B., Goetz, A.F.H., 1993. Derivation of scaled surface reflectances from AVIRIS data. Remote Sens. Environ. 44, 165–178.

Garcia, R., Lee, Z., Hochberg, E., 2018. Hyperspectral shallow-water remote sensing with an enhanced benthic classifier. Remote Sens. 10, 147. https://doi.org/10.3390/rs10010147.

Goodman, J.A., Ustin, S.L., 2007. Classification of benthic composition in a coral reef environment using spectral unmixing. J. Appl. Remote. Sens. 1, 11501. https://doi.org/10.1117/1.2815907.

Goodman, J.A., Purkis, S.J., Phinn, S.R., 2013. Coral Reef Remote Sensing. A Guide for Mapping, Monitoring and Management. Springer, Dordrecht. https://doi.org/10.1007/978-90-481-9292-2.

Hedley, J.D., Mumby, P.J., Joyce, K.E., Phinn, S.R., 2004. Spectral unmixing of coral reef benthos under ideal conditions. Coral Reefs 23, 60–73. https://doi.org/10.1007/s00338-003-0354-x.

Hedley, J., Roelfsema, C., Phinn, S.R., 2009. Efficient radiative transfer model inversion for remote sensing applications. Remote Sens. Environ. 113, 2527–2532. https://doi.org/10.1016/j.rse.2009.07.008.

Hedley, J.D., Roelfsema, C.M., Phinn, S.R., Mumby, P.J., 2012. Environmental and sensor limitations in optical remote sensing of coral reefs: implications for monitoring and sensor design. Remote Sens. 4, 271–302. https://doi.org/10.3390/rs4010271.

Hedley, J.D., Roelfsema, C.M., Chollett, I., Harborne, A.R., Heron, S.H., Weeks, S.J., Skirving, W.J., Strong, A.E., Eakin, C.M., Christensen, T.R.L., Ticzon, V., Bejarano, S., Mumby, P.J., 2016. Remote sensing of coral reefs for monitoring and management: a review. Remote Sens. 8, 118. https://doi.org/10.3390/rs8020118.

Hochberg, E.J., Atkinson, M.J., 2000. Spectral discrimination of coral reef benthic communities. Coral Reefs 19, 164–171. https://doi.org/10.1007/s003380000087.

Hochberg, E.J., Atkinson, M.J., 2003. Capabilities of remote sensors to classify coral, algae, and sand as pure and mixed spectra. Remote Sens. Environ. 85, 174–189. https://doi.org/10.1016/S0034-4257(02)00202-X.

Hochberg, E.J., Atkinson, M.J., Andre, S., 2003. Spectral reflectance of coral reef bottom-types worldwide and implications for coral reef remote sensing. Remote Sens. Environ. 85, 159–173. https://doi.org/10.1016/S0034-4257(02)00201-8.

Hochberg, E.J., Atkinson, M.J., Apprill, A., Andréfouët, S., 2004. Spectral reflectance of coral. Coral Reefs 23, 84–95. https://doi.org/10.1007/s00338-003-0350-1.

Hochberg, E.J., Roberts, D.A., Dennison, P.E., Hulley, G.C., 2015. Special issue on the Hyperspectral Infrared Imager (HyspIRI): Emerging science in terrestrial and aquatic ecology, radiation balance and hazards. Remote Sens. Environ. 167, 1–5. https://doi.org/10.1016/j.rse.2015.06.011.

Holden, H., LeDrew, E., 1998. Spectral discrimination of bleached and healthy submerged corals based on principal component analysis. Remote Sens. Environ. 224, 177–185.

Holden, H., Ledrew, E., 1999. Hyperspectral identification of coral reef features. Int. J. Remote Sens. 20, 2545–2563. https://doi.org/10.1080/014311699211921.

Holden, H., LeDrew, E., 2002. Measuring and modeling water column effects on hyperspectral reflectance in a coral reef environment. Remote Sens. Environ. 81, 300–308. https://doi.org/10.1016/S0034-4257(02)00007-X.

Hughes, T.P., 1994. Catastrophes, phase shifts, and large-scale degradation of Caribbean coral reef. Science 265, 1547–1551.

Jompa, J., McCook, L.J., 2003. Coral-algal competition: macroalgae with different properties have different effects on corals. Mar. Ecol. Prog. Ser. 258, 87–95. https://doi.org/10.3354/meps258087.

Kayal, M., Vercelloni, J., Lison de Loma, T., Bosserelle, P., Chancerelle, Y., Geoffroy, S., Stievenart, C., Michonneau, F., Penin, L., Planes, S., Adjeroud, M., 2012. Predator Crown-of-Thorns starfish (Acanthaster planci) outbreak, mass mortality of corals, and cascading effects on reef fish and benthic communities. PLoS One 7, e47363. https://doi.org/10.1371/journal.pone.0047363.

Kinzie, R.A., Jokiel, P.L., York, R., 1984. Effects of light of altered spectral composition on coral zooxanthellae associations and on zooxanthellae *in vitro**. Mar. Biol. 78, 239–248. https://doi.org/10.1038/470444a.

Kirk, J.T.O., 1994. Light and Photosynthesis in Aquatic Ecosystems. Cambridge. University Press.

Kleypas, J.A., McManus, J.W., Meñez, L.A.B., 1999. Environmental limits to coral reef development: where do we draw the line? Am. Zool. 39, 146–159.

Kutser, T., Dekker, A.G., Skirving, W., 2003. Modeling spectral discrimination of Great Barrier Reef benthic communities by remote sensing instruments. Limnol. Oceanogr. 48, 497–510. https://doi.org/10.4319/lo.2003.48.1_part_2.0497.

Lee, Z., Carder, K.L., Mobley, C.D., Steward, R.G., Patch, J.S., 1999. Hyperspectral remote sensing for shallow waters: 2 deriving bottom depths and water properties by optimization. Appl. Opt. 38, 3831. https://doi.org/10.1364/AO.38.003831.

Lee, C.M., Cable, M.L., Hook, S.J., Green, R.O., Ustin, S.L., Mandl, D.J., Middleton, E.M., 2015. An introduction to the NASA Hyperspectral InfraRed Imager (HyspIRI) mission and preparatory activities. Remote Sens. Environ. 167, 6–19. https://doi.org/10.1016/j.rse.2015.06.012.

Louda, J.W., Li, J.I.E., Liu, L.E.I., Winfree, M.N., Baker, E.W., 1998. Chlorophyll-*a* degradation during cellular senescence and death. Org. Geochem. 29, 1233–1251.

Lubin, D., Li, W., Dustan, P., Mazel, C.H., Stamnes, K., 2001. Spectral signatures of coral reefs: features from space. Remote Sens. Environ. 75, 127–137. https://doi.org/10.1016/S0034-4257(00)00161-9.

McCook, L.J., 1999. Macroalgae, nutrients and phase shifts on coral reefs: scientific issues and management consequences for the Great Barrier Reef. Coral Reefs 18, 357–367. https://doi.org/10.1007/s003380050213.

Meyer, T., Okin, G.S., 2015. Evaluation of spectral unmixing techniques using MODIS in a structurally complex savanna environment for retrieval of green vegetation, non-photosynthetic vegetation, and soil fractional cover. Remote Sens. Environ. 161, 122–130. https://doi.org/10.1016/j.rse.2015.02.013.

Mobley, C.D., Sundman, L.K., Davis, C.O., Bowles, J.H., Downes, T.V., Leathers, R.A., Montes, M.J., Bissett, W.P., Kohler, D.D.R., Reid, R.P., Louchard, E.M., Gleason, A., 2005. Interpretation of hyperspectral remote-sensing imagery by spectrum matching and look-up tables. Appl. Opt. 44, 3576. https://doi.org/10.1364/AO.44.003576.

Mumby, P.J., Green, E.P., Edwards, A.J., Clark, C.D., 1997. Coral reef habitat mapping: how much detail can remote sensing provide? Mar. Biol. 130, 193–202. https://doi.org/10.1088/1361-6382/aa7011.

Mumby, P.J., Steneck, R.S., Hastings, A., 2013. Evidence for and against the existence of alternate attractors on coral reefs. Oikos 122, 481–491. https://doi.org/10.1111/j.1600-0706.2012.00262.x.

National Academies of Sciences, Engineering, and Medicine, 2018National Academies of Sciences, Engineering, and Medicine,. Thriving on Our Changing Planet: A Decadal Strategy for Earth Observation from Space. The National Academies Press, Washington, DC. https://doi.org/10.17226/24938.

Ogston, A.S., Storlazzi, C.D., Field, M.E., Presto, M.K., 2004. Sediment resuspension and

transport patterns on a fringing reef flat, Molokai, Hawaii. Coral Reefs 23, 559–569. https://doi.org/10.1007/s00338-004-0415-9.
Okin, G.S., Gu, J., 2015. The impact of atmospheric conditions and instrument noise on atmospheric correction and spectral mixture analysis of multispectral imagery. Remote Sens. Environ. 164, 130–141. https://doi.org/10.1016/j.rse.2015.03.032.
Okin, G.S., Clarke, K.D., Lewis, M.M., 2013. Comparison of methods for estimation of absolute vegetation and soil fractional cover using MODIS normalized BRDF-adjusted reflectance data. Remote Sens. Environ. 130, 266–279. https://doi.org/10.1016/j.rse.2012.11.021.
Phinn, S.R., Dekker, A.G., Brando, V.E., Roelfsema, C.M., 2005. Mapping water quality and substrate cover in optically complex coastal and reef waters: an integrated approach. Mar. Pollut. Bull. 51, 459–469. https://doi.org/10.1016/j.marpolbul.2004.10.031.
Purkis, S.J., Gleason, A.C.R., Purkis, C.R., Dempsey, A.C., Renaud, P.G., Faisal, M., Saul, S., Kerr, J.M., 2019. High-resolution habitat and bathymetry maps for 65,000 sq. km of Earth's remotest coral reefs. Coral Reefs 38, 467–488. https://doi.org/10.1007/s00338-019-01802-y.
Roberts, D., Gardner, M., Church, R., Ustin, S., Scheer, G., Green, R.O., 1998. Mapping chaparral in the Santa Monica Mountains using multiple endmember spectral mixture models. Remote Sens. Environ. 65, 267–279.
Rogers, C., 1990. Responses of coral reefs and reef organisms to sedimentation. Mar. Ecol. Prog. Ser. 62, 185–202. https://doi.org/10.3354/meps062185.
Rogers, C.S., Miller, J., 2006. Permanent "phase shifts" or reversible declines in coral cover? Lack of recovery of two coral reefs in St. John, US Virgin Islands. Mar. Ecol. Prog. Ser. 306, 103–114. https://doi.org/10.3354/meps306103.
Russell, B., Dierssen, H., LaJeunesse, T., Hoadley, K., Warner, M., Kemp, D., Bateman, T., 2016. Spectral reflectance of Palauan reef-building coral with different symbionts in response to elevated temperature. Remote Sens. 8, 164. https://doi.org/10.3390/rs8030164.
Russell, B., Dierssen, H., Hochberg, E., 2019. Water column optical properties of Pacific coral reefs across geomorphic zones and in comparison to offshore waters. Remote Sens. 11, 1757. https://doi.org/10.3390/rs11151757.
Savitsky, A., Golay, M.J.E., 1964. Smoothing and differentiation of data by simplified least squares procedures. Anal. Chem. 36, 1627–1639.
Siegel, D.A., Maritorena, S., Nelson, N.B., Hansell, D.A., Lorenzi-Kayser, M., 2002. Global distribution and dynamics of colored dissolved and detrital organic materials. J. Geophys. Res. 107https://doi.org/10.1029/2001JC000965. 21-1-21–14.
Smith, J.E., Brainard, R., Carter, A., Grillo, S., Edwards, C., Harris, J., Lewis, L., Obura, D., Rohwer, F., Sala, E., Vroom, P.S., Sandin, S., 2016. Re-evaluating the health of coral reef communities: baselines and evidence for human impacts across the central pacific. Proc. R. Soc. B Biol. Sci. 283, 1–9. https://doi.org/10.1098/rspb.2015.1985.
Somers, B., Asner, G.P., Tits, L., Coppin, P., 2011. Endmember variability in spectral mixture analysis: a review. Remote Sens. Environ. 115, 1603–1616. https://doi.org/10.1016/j.rse.2011.03.003.
Stephens, F.C., Louchard, E.M., Reid, R.P., Maffione, R.A., 2003. Effects of microalgal communities on reflectance spectra of carbonate sediments in subtidal optically shallow marine environments. Limnol. Oceanogr. 48, 535–546. https://doi.org/10.4319/lo.2003.48.1_part_2.0535.
Storlazzi, C.D., Ogston, A.S., Bothner, M.H., Field, M.E., Presto, M.K., 2004. Wave- and tidally-driven flow and sediment flux across a fringing coral reef: Southern Molokai, Hawaii. Cont. Shelf Res. 24, 1397–1419.
Stumpf, R.P., Holderied, K., Sinclair, M., 2003. Determination of water depth with high-resolution satellite imagery over variable bottom types. Limnol. Oceanogr. 48, 547–556. https://doi.org/10.4319/lo.2003.48.1_part_2.0547.
Thompson, D.R., Gao, B.C., Green, R.O., Roberts, D.A., Dennison, P.E., Lundeen, S.R., 2015. Atmospheric correction for global mapping spectroscopy: ATREM advances for the HyspIRI preparatory campaign. Remote Sens. Environ. 167, 64–77. https://doi.org/10.1016/j.rse.2015.02.010.
Thompson, D.R., Hochberg, E.J., Asner, G.P., Green, R.O., Knapp, D.E., Gao, B.C., Garcia, R., Gierach, M., Lee, Z., Maritorena, S., Fick, R., 2017. Airborne mapping of benthic reflectance spectra with Bayesian linear mixtures. Remote Sens. Environ. 200, 18–30. https://doi.org/10.1016/j.rse.2017.07.030.
Torres-Pérez, J.L., Guild, L.S., Armstrong, R.A., Corredor, J., Zuluaga-Montero, A., Polanco, R., 2015. Relative pigment composition and remote sensing reflectance of Caribbean shallow-water corals. PLoS One 10, e0143709. https://doi.org/10.1371/journal.pone.0143709.
Tsai, F., Philpot, W., 1998. Derivative analysis of hyperspectral data. Remote Sens. Environ. 66, 41–51. https://doi.org/10.1016/S0034-4257(98)00032-7.
Vermeij, M.J.A., Dailer, M.L., Smith, C.M., 2011. Crustose coralline algae can suppress macroalgal growth and recruitment on Hawaiian coral reefs. Mar. Ecol. Prog. Ser. 422, 1–7. https://doi.org/10.3354/meps08964.
Vermote, E.F., Tanré, D., Deuze, J.L., Herman, M., Morcette, J.J., 1997. Second simulation of the satellite signal in the solar spectrum, 6s: an overview. IEEE Trans. Geosci. Remote Sens. 35, 675–686.
Willmott, C.J., Matsuura, K., 2005. Advantages of the mean absolute error (MAE) over the root mean square error (RMSE) in assessing average model performance. Clim. Res. 30, 79–82. https://doi.org/10.3354/cr00799.